Crystal Growth Habits of DNA Fractions. 2. Low-Voltage SEM and TEM Examination of Lamellar Structure and Growth Fronts

Kenneth Monar* and Paul J. Phillips†

Department of Materials Science and Engineering, The University of Tennessee, 434 Dougherty Engineering Bldg., Knoxville, Tennessee 37996-2200

Received March 9, 1999; Revised Manuscript Received June 28, 1999

ABSTRACT: In a previous publication we reported the first documentation of the crystal growth habits in a polydisperse, heterogeneous DNA fraction of reasonable molecular weights under quiescent and isothermal conditions. In the relative humidity (RH) range where the A-DNA helix conformation is adopted, these morphologies could best be described as sheaves and spherulites. Here, we extend those light microscopic observations to the nanoscale, with the following conclusions: (1) the growth habit of A-DNA is lamellar with chain (helix) folding, exhibiting the formation of sheaves consisting of individual lamellae similar to those formed by synthetic semicrystalline polymers; (2) the lamellar crystals are thinner than the mean molecular length of the DNA fraction; (3) the lamellae exhibit topological differences in their lateral and basal aspects; (4) the lamellar tips are round and thinner than in the lamellar region behind the tips, which appear more faceted and of a different organizational structure; (5) these two zones are associated with a thickening transition zone; and (6) the interfacial zone at the lamellar growth front contains, what appear to be, bundled molecules based on dimensional and functional considerations.

Introduction

The effect of humidity on the conformation and crystal structure of sodium DNA has been documented for over three decades.[1] It consists of a highly crystalline form (A-DNA) in the range 65−92% relative humidity (RH)[2] (depending on base pair content) or a liquid-crystalline-like form (B-DNA) above ca. 92% RH. Recently, the well-known phase diagrams of DNA, and the hysteresis between the dissolution and formation of A-DNA, and B-DNA formation,[2] which is related to the degree of hydration of the DNA molecule,[3] have been given a morphological basis by the authors.[4] In that work, the details of nucleation and growth habit of a polydisperse, heterogeneous DNA fraction of reasonable molecular weight was first reported for demonstrated quiescent conditions, including controlled undercooling. The following observations were readily understandable on the basis of synthetic polymer crystallization behavior:[5,6] (1) The crystal growth rate increases with undercooling, which in this system is related to the relative humidity, through the hydration level of the DNA molecule,[3] affecting the degree of flexibility and the nature of the salt−hydrate formed. (2) The hysteresis in nucleation and dissolution is similar to the well-established behavior of synthetic polymers and suggests the influence of kinetics on growth. (3) The crystal growth habit and primary nucleation behavior closely resemble those of melt-crystallized, synthetic macromolecules. (4) Optical crystallography and small-angle light scattering experiments on A-DNA crystal forms (spherulites) indicated that they are negatively birefringent.[4]

In addition to behavior similar to that of synthetic polymers, several observations were unique:[4] (1) the lack of sheaf nucleation under conditions where sheaves should grow only after self-seeding (the self-seeding was accomplished through a dehydration step where less stable forms nucleate and grow at lower RH, yet can be dissolved at higher RH and with the concomitant nucleation of the sheaves); (2) the observation of what appears to be a cholesteric liquid crystal (LC) to crystal transition, with accompanying sheaf development.

In this paper, the details of the structure of the sheaves grown in hydrated gels, without stress, under conditions of RH where A-DNA conformations have been established, using TEM replication methods and low-voltage SEM (LVSEM), will be reported Since the RH affects growth rates,[7] and a small RH gradient across the gels cannot be ruled out at this stage, the morphology has been probed for conditions representing various crystallization rates (fast, slow, and moderate), following self-seeded nucleation of the sheaves.[4] In addition, unprecedented ultrastructural detail of a sheaf, and of the tips of lamellar growth fronts, during the process of secondary nucleation, is afforded by the vitrification of the hydrated films during crystallization and low-temperature replication.

An important factor missing in many earlier condensed matter studies of DNA is the role of kinetics in solidification and crystallinity on bulk sample properties. Thus, early work regarding the crystal structure of DNA[8] often relied on orientation induced by stretching or "stroking" fibers or films from DNA of ill-defined molecular weight. The hysteresis in formation and dissolution suggested by ref 2 was found to be morphologically based[4] and indicates the importance of defining the crystallization/dissolution history. Other variance in observations may involve the different comonomer distributions found in the starting materials, complexation of DNA with proteins which affect tertiary structure, and changes in flexibility and secondary structure accompanying changes in RH utilized to induce crystallization. Some historical reference is now considered.

Historically, the first evidence for a folded chain (low order) crystal habit of DNA came from "fibers" of oriented, intact viruses,[10] in which it was demonstrated that the DNA helices are directed normal to the

† To whom all correspondence should be addressed.
* Current address: Oak Ridge National Laboratory, 4500 No., C8, MS 6197, Oak Ridge, TN 37831.

10.1021/ma990360a CCC: $18.00
Published on Web 08/18/1999

principal axis of the virus (thin direction) and must be substantially folded. However, it was workers at Bell Laboratories,[11] working on salmon sperm DNA, who first uncovered the hallmarks of the crystal growth process by growing single crystals from dilute solutions. Nucleation, faceted crystal growth, and molecular weight fractionation relative to the mother liquor were shown. The mean molecular weight from the dissolved crystals exhibited selectivity for the longer molecules. Chain-folded crystal growth was also inferred as the origin of the substantial decrease in long-range order in the single crystals of higher molecular weight calf thymus DNA, as compared to those grown from oligonucleotides,[12,13] and for the evolution of enzyme-vulnerable sites in DNA from longer fragments (>600 base pairs, bp), but not 200−400 bp.[14] At 100% RH the principal reflection from the WAXS indicated intermolecular distances in the virus results[11] which are in line with the B-DNA hexagonal crystals (23.8 Å; refs 11−13) and asymptotically approach values characteristic of A-DNA[23] with decreasing RH. The domain size from line width analysis for the virus WAXS reflections normal to the helix axis (119−143 Å) is similar to that of crystals grown from dilute solution (150 Å) along the helix axis.[11]

The chain-folded nature of the Giannonni crystals[11] was challenged in another study[15] which used a different source of DNA, calf thymus DNA. Hexagonal crystals, with both left- and right-handed screw dislocations, were observed, and crystal thicknesses were ca. 1000 Å. (Strands were either fully extended or once folded.) While the molecular weight and supersaturation conditions were comparable, additional preparative steps related to the freeze fracture method were not verified for changes, and dissolution warranted higher concentrations of nonsolvent. The question of chain folding remained unresolved. However, it is worth noting that calf thymus DNA has a GC content (comonomer) near the lower limit for A-DNA formation,[3] and salmon sperm DNA has a GC content some 10% lower in this fraction.[16] This is manifest by the slightly higher helix → coil transition of the calf thymus study. In both studies, workers found it useful to induce single-crystal formation near the helix → coil transition temperature (presumably introducing a greater degree of chain flexibility by reducing the number of hydrogen bonds bridging the dimer[9]).

The persistence length (l_p) of DNA in dilute solutions is ca. 500 Å or ca. 150 bp,[17] and the statistical (Kuhn) segment length is twice the persistence length.[18] In reality, there is an electrostatic interaction contribution to the persistence length,[19] and it may be close to 380 Å at high salt concentrations.[20] Proteins (histones) may be associated with DNA forming a complex (nucleosome), from which other tertiary and quaternary structures of DNA develop. DNA in these self-condensed states is called chromatin and is often depicted as superhelices of various widths of 100−600 Å as well as a "beads-on-a-string" texture.[9]

Nucleosomes have been used to isolate regular, monodisperse, 146 bp DNA fragments. This persistence length DNA exhibits a liquid to liquid-crystalline (LC) phase transition[21] at critical concentrations consistent with Flory's analysis.[22] NMR and light microscopy have been used to study the liquid-crystalline textures in concentrated solutions for counterion concentrations below 0.2 M.[23,24] The most concentrated solutions yielded a columnar hexagonal LC phase above 350 mg of DNA/mL,[25] which was not smectic.[23] B-DNA structure was observed for the highest concentration having a lattice spacing of 28 Å, which compares with one observed for B-DNA fiber conditions.[26] The generalization of the importance of LC states in-vivo in eukaryotic DNA was reinforced by comparative in-vitro microscopic examinations of DNA in organisms lacking histones.[27] This LC packing was suggested to be similar to deproteinated, high molecular weight DNA from mammalian spermatozoa[28] but differed morphologically from the in-vivo ultrastructure prior to treatment.[29]

A large body of literature has been devoted to DNA condensed states produced using volume exclusion plus salt,[30] ethanol plus salt,[31] or polybasic amino acids[32] and referred to as Ψ-DNA. Under precipitation conditions, inter- and intramolecular collapse are in competition,[33] suggesting the possibility of kinetic influence on the results. Spherulites were reported in solutions,[30] but microscopy indicated LC textures. Precipitation using the volume exclusion effect (which may favor intermolecular condensation) generates crystallographic long-range order.[34] Use of salt and ethanolic solutions (which may favor inter- or intramolecular collapse depending on conditions[31]) produces lower order structures.[14,34]

DNA physical studies have been reported on the basis of the production of fibers from ultrahigh molecular weight calf thymus DNA via wet spinning.[35] These fibers have been extensively studied and reviewed.[36] Upon dissolution, a loss in orientation[37] followed by resolidification did not yield definitive crystal growth processes as we have shown.[4] Consideration of semicrystallinity[4] is important for the interpretation of bulk properties,[38] especially with respect to the noncrystalline material as some data indicate that the conformation of noncrystalline DNA, at A-DNA hydration levels, may be in the B-DNA conformation.[39,40]

In view of the above, a method was developed[4] that followed a middle course, between the oligonucleotides and nucleosome fragments, too short to behave as macromolecules when they crystallize, and ultrahigh molecular weight DNA, whose molecular weight can be so extreme as to wholly inhibit crystal growth relative to primary nucleation. As in the single-crystal studies mentioned above,[11,15] no additional steps to remove associated proteins were performed, and molecular weight reduction to narrow fractions was facilitated through ultrasonic treatment of solutions. Nucleation and growth at ambient temperatures were facilitated by a special microscope cell,[7] which could rapidly hydrate/dehydrate free surface thin films.

We now consider the fine structure of the A-DNA crystals shown in the first paper in this series.[4] The targeted molecular weights were chosen to be 3−4 Kuhn statistical segments, substantially larger than the persistence length and sufficient for wormlike chain behavior. In this regard, it should be recalled that kinetics and not polydispersity are the origins of lamellar crystal growth in synthetic, semicrystalline macromolecules.[6]

Experimental Section

Preparation of Specimens. The study material was a heterogeneous, mammalian DNA obtained commercially (Sigma type 1, D-1501). Preparative methodology regarding the solubilization, molecular weight reduction and characterization, fractionation, and yield estimates was described in the previous report.[4] The molecular weight distribution was determined from micrographs of the toluidine blue-stained gels of the

Table 1. Physical Properties of the DNA

	M_n	M_w	PD
molar mass (g/mol)	676800	945500	1.4
base pairs	1025	1428	
end-to-end (Å)	2666	3712	
no. persistence lengths at 500 Å/l_p (ref 7)	5.0	7.4	
no. persistence lengths at 380 Å/l_p (ref 34)	7.0	9.8	

fractionated DNA together with internal standards.[4] The staining time determined the staining intensity, and it was difficult to obtain good resolution of the peak value, without the tails being of low intensity. In our previous analysis, analytical forms for the molecular weight standard (discrete) and the intensity distribution of the fraction were used to model the data. A reanalysis of that data using an improved method was performed to better characterize the distribution shown in Table 1 and indicates a mean molecular length of 5−7 persistence lengths (l_p) and a polydispersity of 1.4.

The crystallization proceeded via the dissolution of the highly branched spherulitic forms, as described earlier (cf. Figure 8.B, ref 4), followed by recrystallization of sheaves under A-DNA RH conditions (cf. Figure 8.F, ref 4), in the range 3−4 M Na^+.

Electron Microscopy. Low-voltage scanning electron microscopy of untreated dried films was performed using a Hitachi S-900 LV-SEM at 10 keV. Three preparations were examined: (1) The most rapid crystallization of the sheaves was induced by pumping dry air into the sample cell once primary nuclei were observed and placing the film upon a drop of silver paint. (2) Fully crystallized films produced at 87% RH, where the growth was much slower,[1] were studied. (3) Observation of a sheaf nucleus was facilitated by rapid hydration through the RH range where the sheaves were nucleated to moderately high RH, followed by rapid drying.

TEM studies were designed to facilitate observations of the crystallization process in these hydrated gels unaffected by the drying process. The samples were chosen from moderate growth rates between the extremes observed under the SEM conditions. The free surface films were rapidly transferred to gold planchets and rapidly frozen in liquid nitrogen cooled liquid ethane. The planchets were transferred to a liquid N_2-cooled coating stage within Balzers BAF 400T freeze-fracture apparatus. The device was evacuated and cooled to 170 K. The two planchets were rapidly separated and immediately coated with ca. 20 Å of platinum/carbon, followed by coating with ca. 200 Å of carbon using stage rotation. (The layer thickness was controlled with a calibrated piezoelectric device.) The stage was slowly warmed to ambient temperature, and the replicas were floated off the planchets using glass-distilled H_2O. They were observed directly after drying or after floating upon a 10% bleach solution in an attempt to remove any additional organic material. The transmission electron microscopy (TEM) of the replicas was performed using a Hitatchi H-800. Examination of the planchet surfaces indicated that fracture was rare, due to poor adhesion, yet sufficient material was removed and/or the films sufficiently lacy to facilitate observations of the lamellae in bold relief.

Results

A typical 200−300 μm sheaf as observed in the light microscope is shown in Figure 1A. A SEM micrograph of dried films containing these sheaves grown at high crystallization rates appears in Figure 1B, and the sheaves can be seen to be constructed of many individual crystals. When the specimen film is rapidly crystallized, the lamellae are nearly as broad as they are thick and show a tendency for bundling or growth in cells (Figure 2A). Nominal dimensions of the crystals are ca. 700 Å thick. Although some thicker structures can be observed, they cannot be identified as individual or tightly stacked lamella at this magnification. Figure 2B shows details of the region indicated at lamellar bundle 1 in Figure 2A, specifically at the region indicated by an asterisk. The enlargement of this region in Figure 2B reveals a 90 nm wide cylindrical entity, which appears to be uncoiling into fine strands ca. 8 nm in width or diameter (fore and aft; see arrows) while condensed on the lamella (or trapped between lamella).

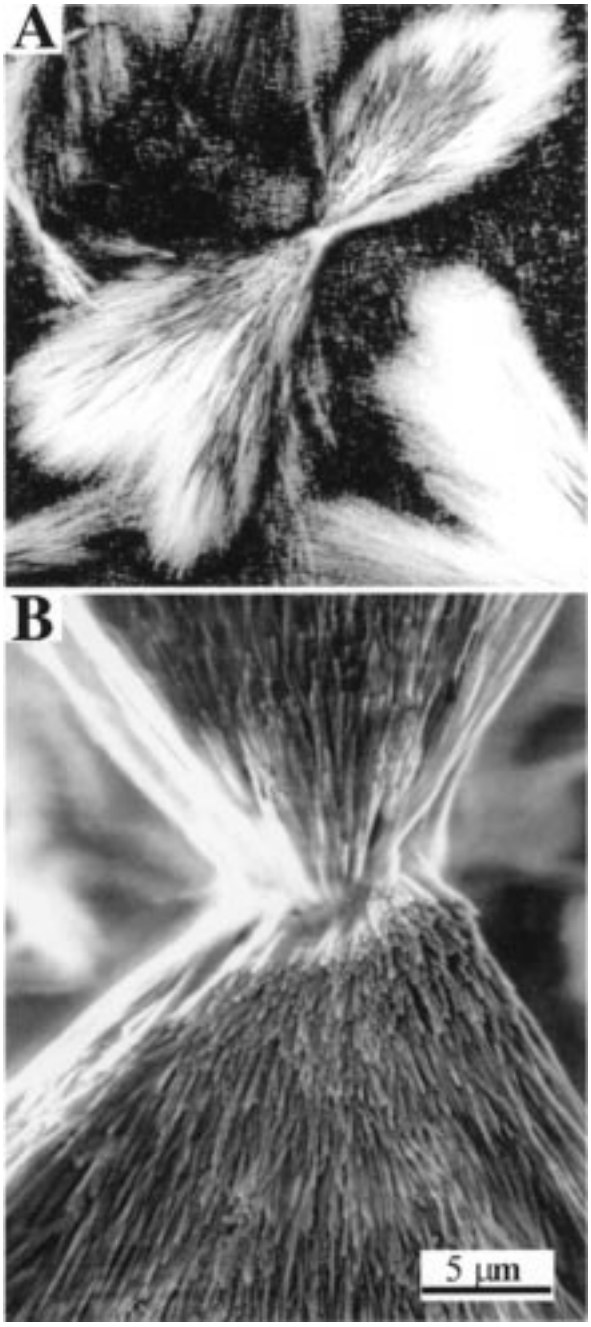

Figure 1. Sheaf habit in DNA gels resulting from rapid crystal growth during rapid dehydration: (A) light microscopy; (B) direct SEM observation from dehydrated films.

Once nucleated, if a specimen was rapidly dehydrated, occasional observation of the initial sheaf nucleus (Figure 3A) could be made (growth conditions expected to be transient). The crystal appears to grow from a central region from which two lamellae emanate, rotated by some angle relative to each lamella's basal plane. Figure 3B (inset) shows an optical micrograph of the early stages of sheaf growth. In Figure 3, the dried gel contains "nodules" which appear as white dots in the micrograph (also observed on the lamellar sheaves in Figure 2A). The tips of the sheaf nucleus of Figure 3 are shown at higher magnification in Figure 4A,B and

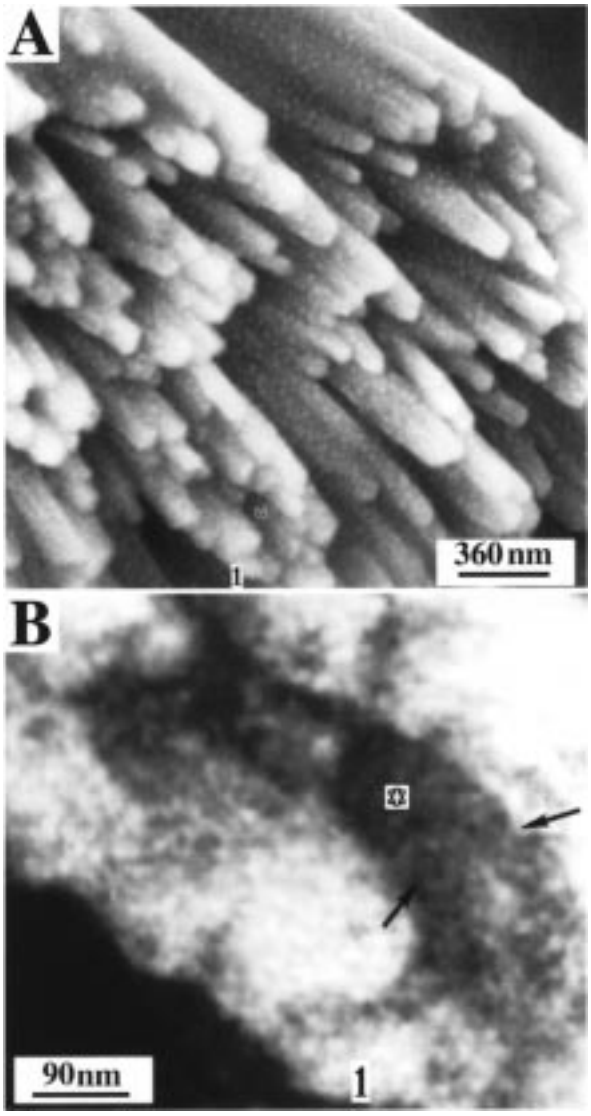

Figure 2. SEM details of the lamellar habit in sheaves from dehydrated films as shown in Figure 1. (A) Habit for rapid crystal growth during rapid dehydration reveals tendency to form stacks with thicknesses approximately equal to widths. (B) Shows region marked 1 in (A) with an asterisk on the lamellae surface indicating the presence of fine strands, both for and aft, of the ca. 90 nm wide crystal.

in insets a and b. In Figure 4A and inset a, whispy coils of gel material are discernible near the tip, yet closer to the tip the material appears to be attached. In contrast, Figure 4B and inset b show that the second growth tip of the sheaf nucleus has material connected to one side of the tip, giving rise to a bead-on-a-string appearance which is less discernible near the side of the tip to which it is connected. These "nodules" are likely to be coiled macromolecular material, are ca. 350 Å in width, and are connected to the lamellar surface when viewed at higher magnification (not shown). It is not known whether these "nodules" result from the drying process, but they have similar dimensions to the nodules seen in DNA supercoils (ca. 300 Å at intermediate ionic strength conditions; cf. Figure 5 in ref 41). Nominal dimensions of the lamellae at the growth tips are ca. 640 Å thick and 190 nm wide.

It was noted in the first publication that sheaf growth was very slow at 87% RH and resulted in sheaves that could reach macroscopic dimensions[4] (Figure 5A). The lamellae grow in tightly associated "cells" (cf. Figure G,

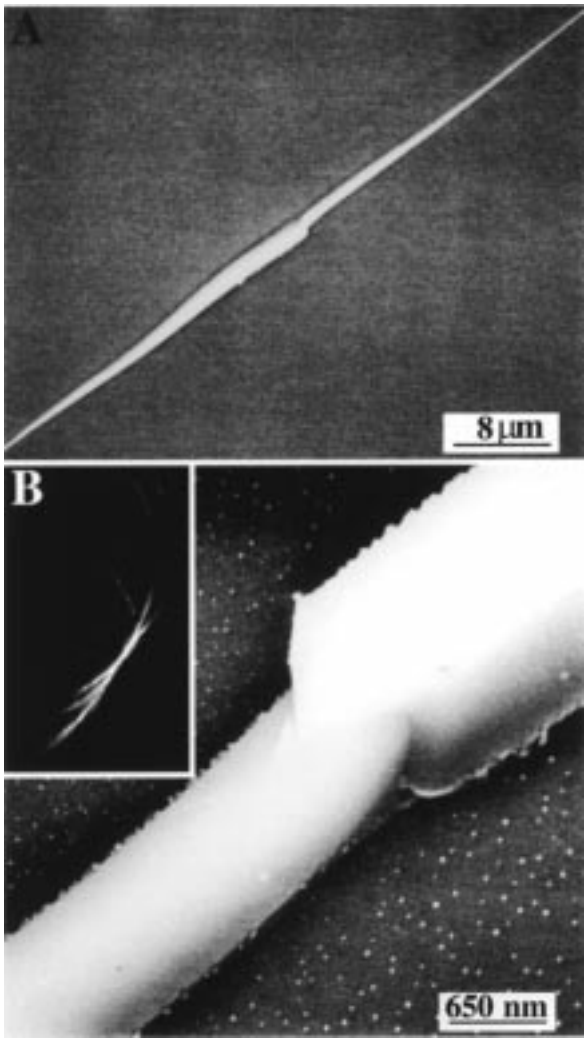

Figure 3. SEM of sheaf homogeneous crystal nucleus (A) and details of the central region (B). Inset shows light micrograph of early stages in sheaf development.

K in ref 4), which can also be seen in the SEM in these fully crystallized films (Figure 5B). The lamellae appear to grow directly from the substrate (in this example, polished Si) in layers. In the region marked 1 the uppermost lamella has a clear faceted growth front. The white arrows in Figure 5B point to strands which can bifurcate and are associated with some growth fronts. Measurements indicate that the strands are 280 Å in diameter prior to an apparent unwinding process (arrows) after which they are ca. 180 Å in diameter. At the region just below the asterisk′ a growth front can be seen having a dendritic projection at the lower edge.

Figure 6A shows a TEM micrograph of a replica of a sheaf growth front vitrified during the crystallization process. The interpretation of regularly patterned objects, in close juxtaposition, was often difficult in the replicas due the three-dimensional relief that is observed in transmission. The growth fronts of the outermost sheaf regions appear to be shadowed from above and are round at the tips. They may contain a transition zone (arrows) that has a less transmissive appearance in the replica and may be in a different plane (suggesting a thickness difference). Sometimes the tips may appear more symmetric (region labeled with an asterisk). The tip region labeled with an asterisk is shown magnified and rotated 90° CCW in Figure 6B. It is uniform along a large portion of its length and shows a

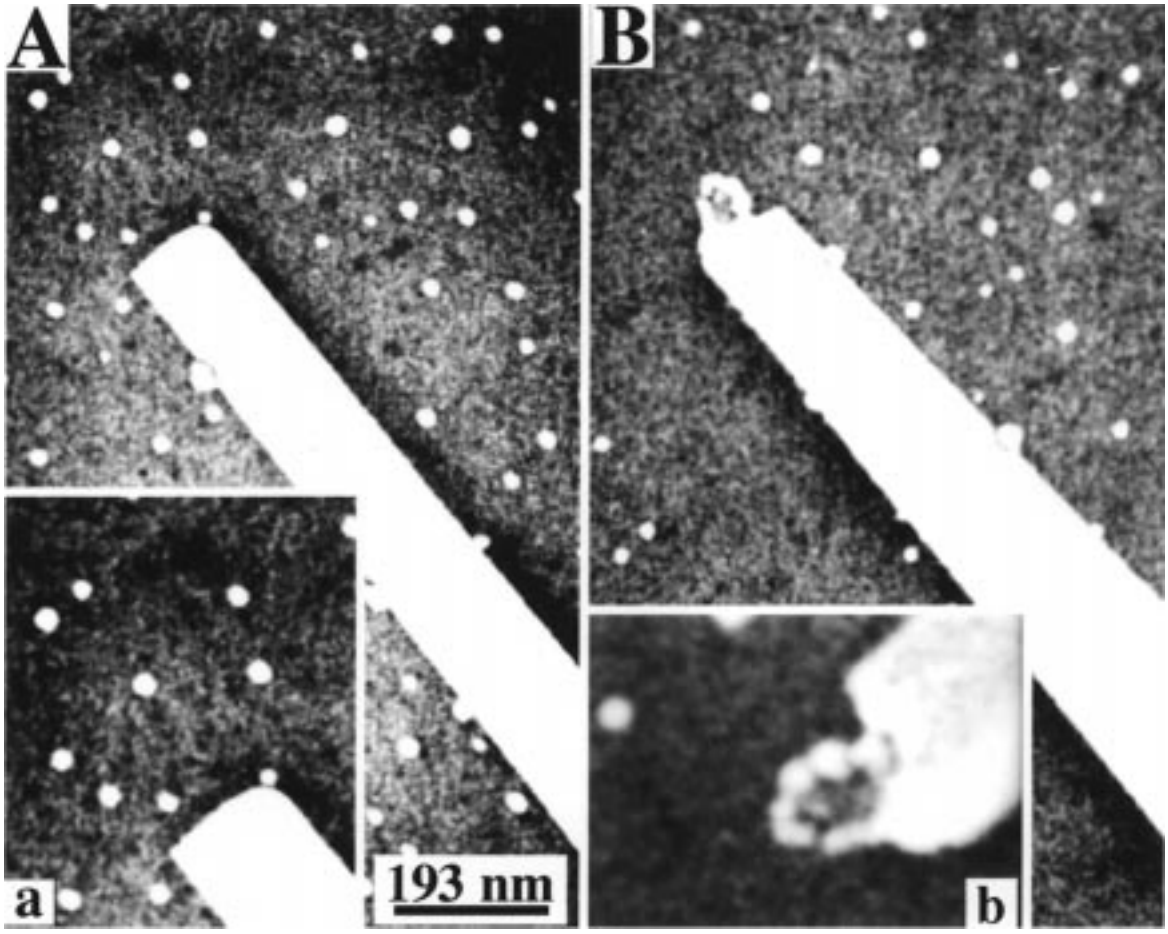

Figure 4. SEM micrograph of the two sheaf nucleus tips and the surrounding dried gel in Figure 3. Inset a shows a tip region with connective strands from the nearby gel. Inset b shows the other tip where a "beads-on-a-string" texture is observed and associated with one edge of the growth front.

clear textural difference between the lateral (L) and basal (B) surfaces. Measurements indicate that both surfaces are composed of long, continuous material ca. 70 Å in diameter (or ca. 2 times the width of the DNA double helix). The lateral portion appears to be comprised of this material in a somewhat more parallel fashion, and it is tilted at ca. 33° to the basal surface normal.

Electron micrographs of lamellae further inward from the sheaf tips (viewed from above) are shown in Figure 7A. Here, the lamellae show a tendency for a ridged habit associated with trailing lamellar growth on one of the lateral sides (see arrows) and showing a significantly different structural view from the sheaf growth front in Figure 6. The growth fronts of the ridged lamella are shown at higher magnification in Figure 7B. Three general observations in the TEM replica studies of the crystal growth fronts were gleaned from extensive observations and are represented by the regions indicated as (i) → (iii) from the growth tip inward to the ridged crystal. These are (i) an outermost fringe, believed to be shadow angle caused by specimen rotation; (ii) a rounded, less ordered tip region which is followed by (iii) a thicker region with a more ordered surface which shows a tendency for facet formation. Enlargement of the region labeled with an asterisk in Figure 7B (inset) may illustrate a filling-in process of two layers (arrows) of the region (iii) from material which would appear to be emanating from the rounded tip zone (ii). Where an angular region (iii) is observed, the region (ii) is seen as displaced approximately to one side of (iii). However, even in adjacent lamellae, the view can differ. The left-most lamella exhibits less of a delineation between zones (ii) and (iii), has a dendritic-like projection, and has an outermost zone (iii) substructure which appears to have partial hexagonal ordering.

The lateral surface of a lamella in the sheaf interior was examined to explore further the details of the interfacial material at the junction of regions (ii) and (iii). Figure 8 shows two 100 nm thick lamellae (labeled 1, 2). On lamella 2, two regions of the interface a and b are indicated, which show features on a molecular level. The general appearance is of stacked layers, initially 20 nm thick furthest from the crystal, and monotonically becoming thicker as the interfacial layers approach the crystal surface. On lamella 2, interfacial region a is shown magnified in inset a. Two arrows focus attention to the original and magnified views in order to discern processes near an active DNA lamellar growth front. The white bar marker in each inset indicates 100 Å. Inset a illustrates a region where looped material sticks out from the plane of the interfacial material, the planes being separated by ca. 75 Å (twice the DNA molecular width). Inset b is an enlargement of region b in lamella 2 (indicated by three horizontal arrows) and shows another example of what is believed to be a uncoiled loop (as in inset a), leaving an intermediate layer position within the interfacial zone and eventually terminating at the crystal surface. Finally, inset c depicts an enlargement of the interfacial zone of lamella 1 and reveals the presence of looped structures (arrows) which are closely associated with a basal surface and

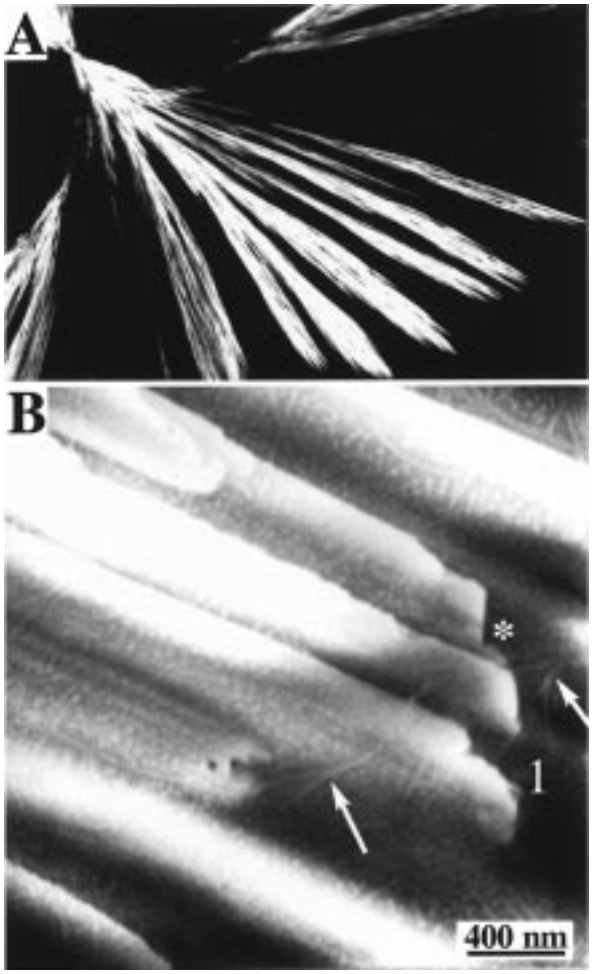

Figure 5. (A) Optical micrograph of slow growing sheaves having lamellae which grow in cells. These cells are evidenced in dried films (B) using SEM and show tightly stacked lamellar growth. The asterisk indicates a growth front with a protuberance, and the arrows show strands of uncoiling of fibrous material. Lamellar front 1 shows a trailing lamellae which appears faceted.

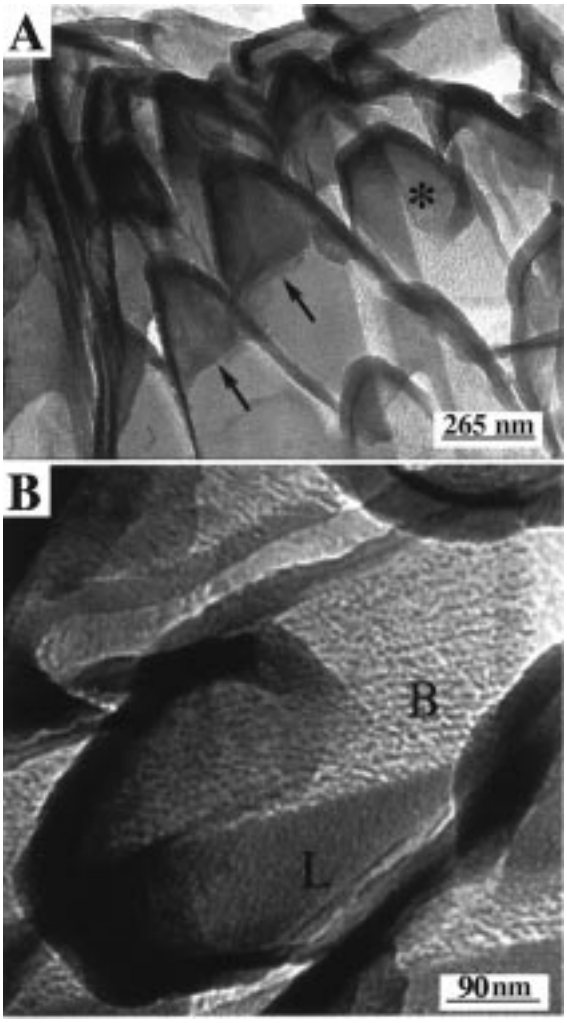

Figure 6. (A) TEM replica of a sheaf growth front crystallized at moderately rapid rates. (B) Detail from the lamellar tip labeled with an asterisk in (A).

are associated with the uncoiling of the 75 Å dimer. The looped structures have a diameter on the order of that of the DNA double helix (ca. 25 Å).

Discussion

These unprecedented observations into the growth of semicrystalline lamellae in fractions of DNA, under conditions leading to A-DNA crystal growth, clearly confirm the lamellar and "helix-folded" habits of growth exhibited by this crystallizable macromolecule, implied in the initial study.[4] Growth of crystals yielded thicknesses of ca. 650−1000 Å, which represent the upper and lower limits to the Kuhn segment length at high and lower counterion concentrations, respectively. Because lower concentrations of counterion represent growth conditions of increasing hydration, we may assume that the stiffness of the DNA molecule has some role in the crystallization process. The growth rates of the DNA crystals shown to have a definitive correlation with morphology at the light microscopic level[4] have now been correlated to the lamellar substructure of the sheaves. The body of results presented must be considered far from complete, tempered by the very complex nature of the undercooling dependencies on concentration of crystallizable species, hydration level, and counterion content. These observations are clearly analogous to many well-established features of the crystallization of synthetic macromolecules.

Two crystal thickness dimensions have been observed with the crystal thickness being thinner for the more rapid growth rates, the rate being inversely related to the RH. The trend is also analogous to synthetic, crystallizable macromolecules as is the disposition of the helix axis with respect to the basal planes of the lamellae. The lamellae vary from isolated crystals with square growth fronts for the most rapid crystallization rates to growth in stacked cells, with reduced nucleation densities, for conditions characteristic of very slow growth rates. The vitrified, growing crystals of Figures 6−8 reveal unique features: (1) rounded retarded growth fronts typically appearing on one facet of a thickened crystal, these having a less ordered appearance than the preceding crystal and a crystal−interface junction exhibiting growth processes described in secondary nucleation theory[42] (Figure 7B); (2) the first observation of tight helix folds associated with ordered basal surfaces from a growth front in the process of solidification; (3) the tips of the crystals at the sheaf growth front (Figure 6) are complex and differ from growth tips within the sheaf (Figures 7 and 8); (4) the presence of multimolecular, or self-condensed, molecules in the crystal growth front zone.

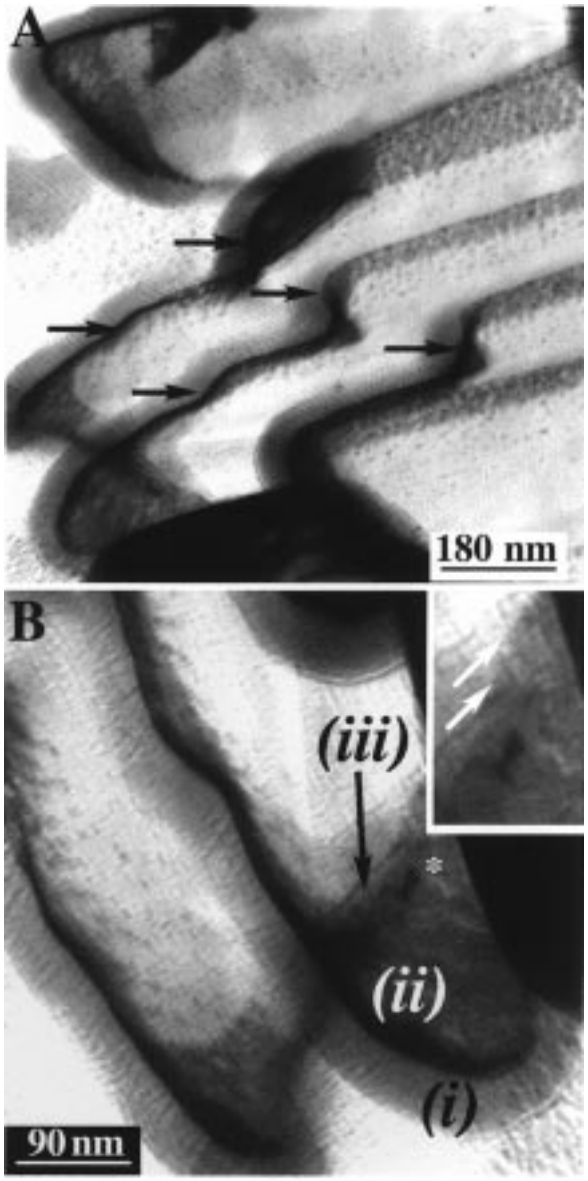

Figure 7. (A) TEM replica of lamellar growth habit away from the leading edges of growth fronts. (B) Enlargement of the fronts of the two lamellae at lower left in (A). The inset serves to illustrate the region labeled with an asterisk which shows the strandlike internal structure of the crystal.

Without improved control of the conditions during its formation, definitive statements regarding the homogeneous sheaf nucleus in Figure 3B cannot be made. Nonetheless, there is a clear presence of angular junctions at the midpoint of the nucleus that are ca. 60° relative to each other. The change in form to a lamellar structure occurs with distance from this junction with considerable thinning (which may be due to changing crystallization conditions). Specimen charging makes it difficult to discern whether or not the crystals are ridged, but the lateral edges are observed in top view in the right-most portion. The edges are featureless near the central junction and then show a serrated pattern with regular spacing. A switchover to the lamellar habit occurs, which may indicate a skeletalization process related to concentration changes such as is well-known in polyethylene.

Comparison of the replicas from the vitrified crystals with images obtained from SEM of dried intact films indicates that the basic crystallizing entity is a 70 Å

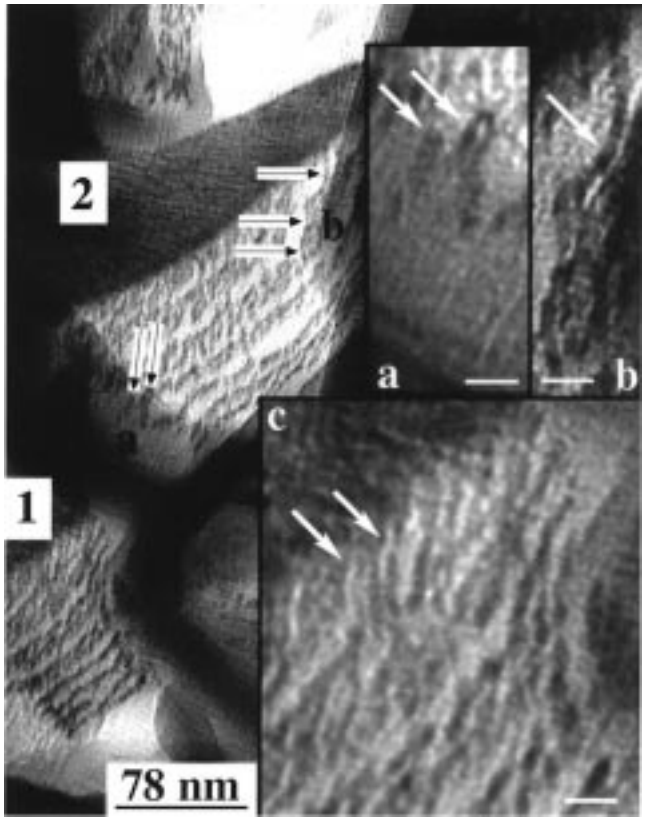

Figure 8. TEM replica of the lateral surfaces of several lamellae. Arrows on lamella 2 indicate two regions (a, b) of the interfacial material which are shown enlarged as insets a and b. Inset c shows details of the interface of the lower lamella. The bars in the insets represent 100 Å.

dimer or self-condensed molecule of the DNA double helix which comprises the rounded growth fronts of the sheaf−gel boundary and can also be observed at the growth fronts of the preferred crystal growth planes, once they have uncoiled. That structure unwinds at the crystal−interface boundary prior to crystallization. The 280 → 180 Å fiber unwinding observed in Figure 5, the 340 Å nodules in Figures 3 and 4, and the 900 Å in Figure 2B must all represent structures formed either in the absence of nucleation or from crystal growth during drying. As similar dimensional forms have all been found in previous works and suggested as resulting from histones,[9] the role of these associated proteins in the crystallization of the DNA helix remains an important complicating factor, which needs to be elucidated.

Perhaps the most controversial observations are those regarding the nature of the rounded growth fronts of DNA lamellar crystals. In polyethylene, the presence of multiple growth sectors in some single crystals was shown to introduce an additional surface strain term causing curved fronts.[43] Simulations have shown that these rounded growth fronts may result from kinetics alone.[44] Simulation has also shown their presence on the preferred growth plane.[45] A lamellar thickening growth (in addition to the familiar lateral growth)[46] in the context of levels of crystalline order[47] may represent an interfacial structure under certain growth conditions. The comparative results of the molecular dimensions at the growth fronts of sheaves, when compared to details of the interfacial structure of crystals in the sheaf interior, would tend to favor the presence of interfacial structure of intermediate order. Whether this is a general feature or a consequence of the gel structure

prior to self-seeded nucleation of spheres is unknown at present.

Conclusions

Studies of the physics of self-assembly in DNA molecules have been shown to benefit from consideration of basic processes in macromolecular crystallization. In turn, the DNA double helix presents polymer physicists with the enigma of a crystallizable polyelectrolyte having a random comonomer sequence, the DNA molecule hiding its irregular primary structure inside the very regular tertiary structure of the double helix: a dimer of two linear, flexible macromolecules. The very thick crystals and the large dimensions of the DNA molecule have provided a unique opportunity to observe some details of the crystallization process and of the molecules at the crystal surfaces, which has not been possible for synthetic macromolecules having molecular cross sections an order of magnitude smaller. In DNA at least, there appears to be some role for multimolecular or self-condensed bundles in the crystallization process which reinforces the observation of the cholesteric → lamellar crystal transformation documented in ref 4.

DNA fractions of M_n 680 000 g/mol and low polydispersity having a mean molecular length of 5−10 persistence lengths form lamellae of ca. 2 persistence lengths in thickness. This fact, together with the microscopic evidence, suggests that the DNA helix is able to form chain folded crystals, similar to synthetic macromolecules crystallized from the melt or solution.[5] An intriguing possibility in this semirigid macromolecule is that diminished stability of the helix at the fold sites is actually coded into the DNA base sequence.

TEM studies have demonstrated the presence of crystal growth processes analogous to those of synthetic macromolecules, including two-dimensional growth, thickening, and folding. A question not addressed in this work is whether the A-conformation is restricted to the crystalline state or whether all molecules (crystalline and noncrystalline) are in this conformation at the indicated RH. The recent demonstration of electrical conduction in DNA[48] should continue to generate interest in the influence of state on physical properties.

These introductory observations of quiescent crystal growth of DNA crystals have explored only a small fraction of the crystal habits observed as a function of RH.[4] Future avenues to consider for these studies are diffraction studies of the structures in this report, microspectrophotometry of gel and crystal states, details of the ultrastructure of the different crystal habits, and the effect of an additional deproteinating step on the morphology. The question of the difference in the crystal thickness in the calf thymus[15] and salmon sperm[11] DNA single-crystal results remains, and this work would suggest that the calf thymus DNA can form crystals on the order of two persistence lengths and in the range of 1000 Å. However, these crystals are chain (helix) folded.

Acknowledgment. The authors acknowledge Dr. David Joy for assistance with the LV-SEM and Dr. J. R. Dunlap for application of the freeze-fracture method and TEM specimen preparative procedures and to the Electron Microscopy Facility at the University of Tennessee. The work was performed with the support from a Research Development Grant from the University of Tennessee.

References and Notes

(1) Holmes, K. C.; Blow, D. M. *The Use of X-ray Diffractions in the Study of Protein and Nucleic Acid Structure*; Wiley-Interscience: New York, 1966.
(2) Pilet, J.; Brahms, J. *Nature* **1972**, *236*, 99.
(3) Falk, M.; Hartman, Jr., K. A.; Lord, R. C. *J. Am. Chem. Soc.* **1963**, *85*, 387.
(4) Monar, K.; Phillips, P. J. *J. Polym. Sci., Polym. Phys. Ed.* **1997**, *35*, 1843.
(5) Bassett, D. C. *CRC Rev. Solid Mater. Sci.* **1984**, *12*, 97.
(6) Phillips, P. J. *Rep. Prog. Phys.* **1990**, *53*, 549.
(7) Monar, K. MS Thesis, The University of Tennessee, 1992.
(8) For the early pioneering work on DNA structure, consult ref 9.
(9) Saenger, W. *Principles of Nucleic Acid Structures*; Springer-Verlag: New York, 1984.
(10) North, A. C. T.; Rich, A. *Nature* **1961**, *191*, 1242.
(11) Giannonni, G.; Padden, F. J.; Keith, H. D. *Proc. Natl. Acad. Sci. U.S.A.* **1969**, *62*, 964.
(12) Downing, K. H.; Glaeser, R. M. *Biophys. J.* **1980**, *32*, 851.
(13) Downing, K. H. *Ultramicroscopy* **1984**, *13*, 35.
(14) Laemmli, U.K. *Proc. Natl. Acad. Sci. U.S.A.* **1975**, *72*, 4288.
(15) Lerman, L. S.; Wilkerson, L. S.; Venable, J. H.; Robinson, B. H. *J. Mol. Biol.* **1976**, *108*, 271.
(16) Fasman, G. *Handbook of Biochemistry and Molecular Biology*; CRC Press: Boca Raton, FL, 1976; Vol. 2.2.
(17) Charney, E. *Q. Rev. Biophys.* **1988**, *21*, 1.
(18) Ullman, R. *J. Chem. Phys.* **1968**, *49*, 5486.
(19) Grosberg, A. Y.; Khokhlov, A. R. *Statistical Physics of Macromolecules*; AIP Press: New York, 1994.
(20) Sobel, E. S.; Harpst, J. A. *Biopolymers* **1991**, *31*, 1559.
(21) Rill, R. L.; Hilliard, Jr., P. R.; Levy, G. C. *J. Biol. Chem.* **1983**, *258*, 250.
(22) Flory, P. J. *Proc. R. Soc. London Ser. A* **1956**, *A234*, 73.
(23) Strzelecka, T. E.; Davidson, M. W.; Rill, R. L. *Nature* **1988**, *331*, 457.
(24) Strzelecka, T. E.; Rill, R. L. *Biopolymers* **1990**, *30*, 57.
(25) Livolant, F.; Levulut, A. M.; Doucet, J.; Benoit, J. P. *Nature* **1989**, *339*, 724.
(26) Franklin, R. E.; Gosling, R. G. *Nature* **1953**, *171*, 740.
(27) Livolant, F. *Eur. J. Cell Biol.* **1984**, *33*, 300.
(28) Livolant, F. *Tissue Cell* **1984**, *16*, 535.
(29) Koehler, J. K.; Wurschmidt, U.; Larsen, M. P. *Gamete Res.* **1983**, *8*, 357.
(30) For review see: Lerman, L. S. In *Physico-Chemical Properties of Nucleic Acids*; Duchesne, J., Ed.; Academic Press: New York, 1973; Vol. 3, p 59.
(31) For example: Huey, R.; Mohr, S. C. *Biopolymers* **1981**, *20*, 2533.
(32) Phillips, C. L.; Mickols, W. E.; Maestre, M. F.; Tinoco, I. *Biochemistry* **1986**, *25*, 7803.
(33) Post, C. B.; Zimm, B. H. *Biopolymers* **1982**, *21*, 2123.
(34) Damaschun, H.; Damaschun, G.; Becker, M.; Buder, E.; Misselwitz, R.; Zirwer, D. *Nucl. Acids Res.* **1978**, *5*, 3801.
(35) Rupprecht, A. *Biotechnol. Bioeng.* **1970**, *12*, 93.
(36) Lindsay, S. M.; Lee, S. A.; Powell, J. W.; Weidlich, T.; DeMarco, C.; Lewen, G. D.; Tao, N. J.; Rupprecht, A. *Biopolymers* **1988**, *27*, 1015.
(37) Lewen, G.; Lindsay, S. M.; Tao, N. J.; Weidlich, T.; Graham, R. J.; Rupprecht, A. *Biopolymers* **1986**, *25*, 765.
(38) Weidlich, T.; Lindsay, S. M.; Rupprecht, A. *Biopolymers* **1987**, *26*, 439.
(39) Brandes, R.; Vold, R. R.; Kearns, D. R. *Biopolymers* **1988**, *27*, 1159.
(40) Fritzsche, H.; Rupprect, A. *J. Mol. Liq.* **1990**, *46*, 39.
(41) Eickbush, T. H.; Moudriankis, E. N. *Cell* **1978**, *13*, 295.
(42) Hoffman, J. D.; Davis, G. T.; Lauritzen, J. I., Jr. In *Solid State Chemistry*; Hannay, N. B., Ed.; Plenum Press: New York, 1976; Vol. 3, p 497.
(43) Miller, R. L.; Hoffman, J. D. *Polymer* **1991**, *31*, 963.
(44) Mansfield, M. L.; Klushin, L. I. *Polymer* **1994**, *35*, 2937.
(45) Yamamoto, T. *J. Chem. Soc., Faraday Trans.* **1995**, *91*, 2559.
(46) Hikosaka, M.; Amano, K.; Rastogi, S.; Keller, A. *Macromolecules* **1997**, *30*, 2067.
(47) Keller, A.; Hikosaka, M.; Rastogi, S.; Toda, A.; Barham, P. J. *J. Mater. Sci.* **1994**, *29*, 2579.
(48) Fink, H.-W.; Schonenberger, C. *Nature* **1999**, *398*, 407.

MA990360A